Infiltration in soils with a saturated surface

W.L. Hogarth[1], D.A. Lockington[2], D.A. Barry[3], M.B. Parlange[3],

R. Haverkamp[4], J.-Y. Parlange[5]

[1] Faculty of Science and IT, The University of Newcastle, Callaghan, NSW, Australia, 2300

[2] School of Civil Engineering and National Centre for Groundwater Research and Training, The University of Queensland, St Lucia, Qld, Australia, 4072

[3] Ecole polytechnique fédérale de Lausanne (EPFL), Faculté de l’environnement naturel, architectural et construit, Institut d’ingénierie de l’environnement, Station no. 2, CH-1015 Lausanne, Switzerland.

[4] University Grenoble 1, CNRS, URA 1512, IMG, LTHE, F-38041, France

[5] Department of Biological and Environmental Engineering, Cornell University, Ithaca, NY, 14853, USA (jp58@cornell.edu)

Abstract: An earlier infiltration equation relied on curve fitting of infiltration data for the determination of one of the parameters, which limits its usefulness in practice. This handicap is removed here and the parameter is now evaluated by linking it directly to soil-water properties. The new predictions of infiltration using this evaluation are quite accurate. Positions and shapes of soil-water profiles are also examined in detail and found to be predicted analytically with great precision.

Keywords: Infiltration in soils, water profiles, constant surface water, Richards equation.

Running title: Infiltration and water profiles.

Introduction and Theoretical Background

The infiltration process of soil enters into most hydrological problems, e.g., irrigation, erosion, and weather forecasting, among many. Physically based infiltration equations go back at least to Green and Ampt (1911) with greater understanding being obtained with Richards equation (1931). Two very thorough reviews of most of the existing infiltration equations based on Richards equation can be found in Basha (2011) and in Triadis and Broadbridge (2010). Those discussions will not be repeated here except when they impact this paper directly.

The present paper continues an approach which is based on Green and Ampt (1911) and Richards equation (1931). Parlange, et al. (1982) introduced a three parameter infiltration equation valid for a saturated soil surface. Those parameters are sorptivity, saturated conductivity and an interpolation parameter δ, which goes from 0, when the equation reduces to Green and Ampt (1911), to 1 when the equation reduces to one obtained earlier by Talsma and Parlange (1972), see also Smith and Parlange (1978). This three parameter equation is discussed in detail by Basha (2011) and Triadis and Broadbridge (2010) following new interpretations. A fourth parameter was introduced by Haverkamp, et al. (1990) to represent ponding on the surface. Barry, et al. (1995) used this fourth parameter, γ, as a curve fitting parameter, but simplified the equation by taking $\delta=1$.

As in Barry, et al. (1995), we keep $\delta=1$ even though values of δ less than one can be used to improve the agreement with numerical results for infiltration (Parlange, et al., 1985; Haverkamp, et al., 1988; Basha, 2011). As this paper concentrates on a discussion of γ, we keep $\delta=1$. In addition, for capillary rise $\delta=1$ (Kunze, et al., 1985), and if δ is a true physical parameter, then the same value should hold for infiltration. However, it is quite easy to reintroduce δ in the equations if so desired.

In a recent paper on time compression approximations (TCA) by Hogarth, et al. (2011), relationships between the cumulative infiltration, I, and the surface flux, q, were examined in details based on an expansion procedure started by Parlange et al. (1997). For the purpose of TCA, it was sufficient to consider the cases when either the surface flux or the surface water content is constant, even though the method can be applied for arbitrary surface conditions. In this paper, we are primarily concerned with infiltration and the profile determination following the same basic procedure (Parlange et al. 1997). The profiles are given by Eq. (1) below, e.g. see Eq. (2) in Hogarth et al. (2011).

$$\int_{\theta}^{\theta_s} \frac{D\,d\bar{\theta}}{q\bar{\theta}/\theta_s - k\left(\bar{\theta}\right)} = z + Mz^2. \qquad (1)$$

Where θ is the water content at vertical position, z, $z = 0$ at the surface with θ_s being the water content at $z = 0$ and time, t. $D(\theta)$ and $k(\theta)$ are the soil-water diffusivity and conductivity, respectively. When $\theta_s = \theta_{sat}$ (the saturated value), M is taken as

$$2\int_0^{\theta_{sat}} D\,d\theta M / q = \int_0^{\theta_{sat}} \left(\theta_{sat} - \theta\right) D\,d\theta \Big/ \int_0^{\theta_{sat}} \theta D\,d\theta. \qquad (2)$$

For q constant, the M-term is negligible (Hogarth et al. 2011, see also Sivapalan and Milly, 1989). For simplicity, we assume that the initial water content, θ_i, can be taken as constant. As a result, θ stands for the water content minus θ_i. Similarly, k and q stand for the conductivity and flux minus the conductivity at θ_i. Taking a non-uniform initial water content introduces complications in writing the equations but with no theoretical difficulties, following the approach of Boulier et al. (1984).

It is important to note that neglecting M for q constant is necessarily approximate as $M = 0$ is exact only when q / θ_s is independent of time (Fleming et al. 1984). There have been many papers exploring the accuracy of Eq. (1) with $M = 0$ for q constant, and possible alternatives to the use of $q\overline{\theta} / \theta_s$ in the integral, e.g., see Kutilek (1980); Boulier et al. (1984); Si and Kachanoski (2000); Evanselides et al. (2005). The conclusion is that in practice, the use of $q\overline{\theta} / \theta_s$ is very accurate, in agreement with the suggestion originally made in Eq. (8) of Parlange (1972), as long as the initial water content is not too large (Boulier et al. 1984).

Fig. 1 summarizes the case considered by Boulier et al. (1984) and Parlange et al. (1985) for q constant using a Grenoble sand whose properties are given in those two papers. The numerical and analytical results are essentially undistinguishable on the figures. This was not the case with Boulier et al. (1984) and Parlange et al. (1985) where numerical results showed dispersion near the wetting front. Here the numerical results were obtained using COMSOL finite element numerical software. This software eliminated the numerical dispersion and thus can be trusted to provide accurate solutions at the wetting front. Note that using Eq. (1) with $\mathrm{M} = 0$ requires the knowledge of $\theta_s(t)$ which is obtained by conservation of mass, integrating Eq. (1) to obtain

$$\int_0^{\theta_s} \frac{D \theta d \theta}{q \theta / \theta_s - k} = qt. \tag{3}$$

Note also that the measured profiles differ slightly from the predicted profiles simply reflecting that the properties, obtained from many experiments, were not exactly those of the particular soil sample used for the experiment in Fig. 1. Experimental scatter of this nature is not unexpected and is sometimes used, wrongly, to justify poor approximate analytical solutions. Rather, analytical approximations should be as accurate as possible so that differences with observations are unambiguously linked to experimental uncertainties and not to inaccurate models. The solution for q constant and $\mathrm{M}=0$ will be used later for comparison to the solution with $\mathrm{M}\neq 0$.

Cumulative Infiltration and Flux with Surface Saturation:

We are now using the profiles with $M\neq 0$, given by Eq. (2) and $\theta_s=\theta_{sat}$. The first step is to derive the equivalent to Eq. (3) to obtain $\mathrm{q}(\mathrm{t})$. Several expressions have been used in the past that related I and q. Eq. (20) of Hogarth et al. (2011) gave

$$\int_0^{\theta_{sat}} \frac{D\theta d\theta}{q\theta/\theta_{sat}-k} = I + \int_0^{\theta_{sat}} \left(\theta_{sat}-\theta\right) D d\theta / 2q. \quad (4)$$

The last term is an approximation of $M\int_0^{\theta_{sat}} z^2 d\theta$ for short times, such that $Iq \simeq S^2/2$, where S is the sorptivity approximated by

$$S^2 \simeq \int_0^{\theta_{sat}} D\left(\theta_{sat}+\theta\right) d\theta. \quad (5)$$

Eq. (4) is identical, with minor notation differences, with Eq. (9) of Parlange et al. (1982). If one ignored the $\mathrm{M}-$term altogether, then the first term in Eq. (4) would have to be corrected for the resulting equation to hold in the short time to obtain Eq. (18) of Barry et al. (2008)

$$\left(S^2/2\theta_{sat}\int_0^{\theta_{sat}} D d\theta\right)\int_0^{\theta_{sat}} \frac{D\theta d\theta}{q\theta/\theta_{sat}-k} = I. \quad (6)$$

Finally, Eq. (6) can be modified to take into account a small negative potential h_{str}, with the soil remaining saturated for $h > -|h_{str}|$. Conceptually, $|h_{str}|$ can be associated with the largest pores in the soil (Haverkamp, et al. 1990). In practice, the value of $|h_{str}|$ cannot be measured independently and instead was obtained by curvefitting infiltration data (Barry et al. 1995). Eq. (6) then becomes

$$\frac{S^2}{2\theta_{sat}\int_0^{\theta_{sat}} D d\theta}(1-\gamma)\int_0^{\theta_{sat}} \frac{D\theta d\theta}{q\theta/\theta_{sat}-k} = I - \frac{\gamma S^2/2}{q-k_{sat}} \qquad (7)$$

where

$$\gamma = -2k_{sat}h_{str}\theta_{sat}/S^2. \qquad (8)$$

Note that in Eq. (7) of Barry et al. (1995) and Eq. (16) of Haverkamp et al. (1990), the equations were further simplified by assuming

$$D/\theta_{sat}\int_0^{\theta_{sat}} D d\theta = d\left(k/\theta\right)/d\theta \big/ k_{sat}. \qquad (9)$$

Since k increases rapidly with θ, k/θ is hardly different from k/θ_s. Making that substitution in Eq. (9) and combining it with $D = kdh/d\theta$, where h is the potential, leads to an exponential dependence of k on h, i.e., the standard Gardner relation. Thus, in our case, Eq. (9) implies a soil hardly different from a Gardner soil. It is clear that eliminating D from the integral of Eq. (7), using Eq. (9), results in an integral, where k/θ is the variable, which can be integrated explicitly as done by Barry et al. (1995) and Haverkamp et al. (1990). This simplification will be discussed further later on.

In the present paper, the soil surface is taken at a zero potential. There is no difficulty to include a ponding term $h_{surf} > 0$ which is simply added to $|h_{str}|$ as done in Haverkamp et al. (1990) and Barry et al. (1995). It is not considered here as it corresponds only to changing the value of γ.

Altogether, we consider two possible relations between I and q, Eqs. (4) and (7), which could be simplified using Eq. (9). Eq. (6) is, of course, just Eq. (7) with $\gamma = 0$. Obviously, for the Grenoble sand used for our illustration, $|h_{str}|$ and γ are physically equal to zero. However, Barry et al. (1995) took a non-zero, and hence non-physical, value to improve infiltration prediction keeping γ only as a curve fitting parameter. In the following, we first discuss the results obtained from Eq. (4). Then we follow the same approach starting with Eq. (7) and compare the results.

Since we paid special attention to short time infiltration to obtain Eq. (4), we are first considering the Taylor expansion of the equation for q large, keeping the first two terms only. Eq. (4) yields

$$Iq \simeq S^2 / 2 + \theta_{sat}^2 \int_0^{\theta_{sat}} k\left(D/\theta\right) d\theta / q . \qquad (10)$$

Finally, we can simplify Eq. (4) using Eq. (9) to obtain

$$I = \frac{\theta_{sat} \int_0^{\theta_{sat}} D d\theta}{k_{sat}} \ln \frac{q}{q - k_{sat}} - \int_0^{\theta_{sat}} \left(\theta_{sat} - \theta\right) D d\theta / 2q. \qquad (11)$$

To obtain the relationships between q and t, we differentiate Eq. (4) with respect to time, replacing dI/dt by q, to obtain a differential equation for q which is easily integrated to obtain

$$t = \int_0^{\theta_{sat}} \frac{D\theta^2}{k^2\theta_{sat}} \ln\left(\frac{q\theta/\theta_{sat} - k}{q\theta/\theta_{sat}}\right) d\theta + \int_0^{\theta_{sat}} \frac{D\theta^2 d\theta}{k\theta_{sat}\left(q\theta/\theta_{sat} - k\right)} - \frac{1}{4q^2} \int_0^{\theta_{sat}} (\theta_{sat} - \theta)\, D d\theta \tag{12}$$

and using Eq. (9) in the two integrals so that only k/θ enters as variable we obtain

$$t = \frac{\theta_{sat}\int_0^{\theta_{sat}} Dd\theta}{k_{sat}^2}\left(1n\frac{q}{q-k_{sat}} - \frac{k_{sat}}{q}\right) - \frac{1}{4q^2}\int_0^{\theta_{sat}}\left(\theta_{sat} - \theta\right) Dd\theta. \tag{13}$$

Starting now with Eq. (7), we proceed as before; the Taylor expansion for large q, keeping the first two terms only, or

$$Iq \simeq S^2/2 + \left[\left(S^2/2\theta_{sat}\int_0^{\theta_{sat}} Dd\theta\right)\theta_{sat}^2\int_0^{\theta_{sat}} k\left(D/\theta\right)d\theta\left(1-\gamma\right) + \gamma S^2 k_{sat}/2\right]/q. \tag{14}$$

Note that for $\gamma = 0$, Eqs. (10) and (14) differ by the term

$$1 - \left(S^2/2\theta_{sat}\int_0^{\theta_{sat}} Dd\theta\right) \simeq \int_0^{\theta_{sat}}\left(\theta_{sat} - \theta\right)Dd\theta / 2\int_0^{\theta_{sat}} \theta_{sat} Dd\theta, \tag{15}$$

which is small. In all our estimates, we keep terms up to that small order and ignore terms of higher order, i.e., square terms.

If we use Eq. (9) to estimate the I/q terms in Eq. (14), then Eq. (14) reduces to Eq. (10) if we take

$$\gamma = \gamma_0 = \int_0^{\theta_{sat}}\left(\theta_{sat} - \theta\right)Dd\theta / 2\theta_{sat}\int_0^{\theta_{sat}} Dd\theta. \tag{16}$$

Finally, we simplify Eq. (7) when Eq. (9) holds and obtain

$$I = \frac{S^2}{2k_{sat}}\left(1-\gamma\right)1n\frac{q}{q-k_{sat}} + \frac{\gamma S^2}{2\left(q-k_{sat}\right)}. \tag{17}$$

We now differentiate Eq. (7) with respect to time, and integrate the resulting differential equation to obtain

$$t = \frac{S^2(1-\gamma)}{2\theta_{sat}\int_0^{\theta_{sat}} D d\theta}\left[\int_0^{\theta_{sat}} \frac{D\theta^2}{k^2\theta_{sat}} 1n\left(\frac{q\theta/\theta_{sat}-k}{q\theta/\theta_{sat}}\right)d\theta + \int_0^{\theta_{sat}} \frac{D\theta^2 d\theta}{k\theta_{sat}(q\theta/\theta_{sat}-k)}\right] - \frac{\gamma S^2}{2k_{sat}^2}\left(1n\frac{q}{q-k_{sat}} - \frac{k_{sat}}{q-k_{sat}}\right), \quad (18)$$

and with Eq. (9)

$$t = \frac{S^2}{2k_{sat}^2}\left[(1-2\gamma)1n\frac{q}{q-k_{sat}} - (1-\gamma)\frac{k_{sat}}{q}\right] + \frac{\gamma S^2}{2k_{sat}(q-k_{sat})}. \quad (19)$$

Fig. (2) compares $q(t)$ given by Eqs. (12, 13, 18 and 19) with γ from Eq. (16) equal to 0.05, with the numerical results.

Several results are apparent. First, Eq. (12) provides an excellent approximation for $q(t)$ when compared to the numerical results. The results predicted by Eq. (18) are equally good if we take $\gamma = \gamma_0 = 0.05$ as given by Eq. (16). Interestingly, Eqs. (13) and (19) are still in basic agreement with each other, with γ =0.05, but they differ significantly from the numerical results. This discrepancy simply shows that the Gardner-type relation of Eq. (9) is not exact for the Grenoble sand and, not surprisingly, this assumption affects Eqs. (18) and (18) in a similar manner.

We know (Barry, et al., 1995) that Eq. (19) can be curve fitted accurately, but only by using a γ differently from γ_0. Of course, Eq. (19) is easy to use in practice once γ is known as it relies only on the knowledge of two additional parameters, S and k_{sat} (besides γ), whereas Eq. (12) requires the estimations of two integrals (based on knowing D and k of θ) for each value of the flux q. Furthermore, Eq. (19) can be used easily in the case of infiltration with ponding (Barry, et al., 1995).

The main inconvenience of using Eq. (19) as in Barry, et al. (1995) is that γ in that paper had to be obtained by curve fitting as the theoretical value of Eq. (16) shows poor accuracy, see Fig. (2). Instead, we are now going to estimate a constant value of γ, i.e., independent of the flux, based on soil properties. For that purpose, we first remember that, as shown in Fig. 2, Eq. (7) is in good agreement with both the numeric and Eq. (4) for $\gamma = \gamma_0 = 0.05$. Then, the result for q large, i.e., Eq. (11) with $\gamma = \gamma_0 \left(= 0.05\right)$, is taken as equal to the result for $\gamma \neq \gamma_0$ but obtained when Eq. (9) is used. This straightforward calculation gives

$$\gamma = \frac{2\theta_{sat}}{k_{sat}\int_0^{\theta_{sat}} D d\theta} \int_0^{\theta_{sat}} \frac{kD}{\theta} d\theta \left(1-\gamma_0\right) + 2\gamma_0 - 1. \tag{20}$$

Of course, if Eq. (9) truly holds, Eq. (20) yields $\gamma = \gamma_0$. For our particular example, this gives instead $\gamma = 0.39$ and, as shown in Fig. 3, this value, when used in Eq. (19), gives a very good estimate of $q(t)$ as expected.

To estimate the sensitivity of the results to the value of γ, a slightly different value, $\gamma = 0.33$, is also considered. This value was chosen by curve fitting Eq. (19) to the numerical results for $t \rhd 1000s$, when $\gamma = 0.39$ is not quite as good. However, $\gamma = 0.39$ is clearly better on the average, if we combine Eqs. (17) and (19) to predict $I(t)$, then, as shown in Fig. 4, the choice of $\gamma = 0.39$ is neatly superior to that of $\gamma = 0.33$. Altogether, then, Eq. (20) gives an adequate physical estimate of γ, requiring no curve fitting to predict either $I(t)$ or $q(t)$ with the very simple equations given in Eqs. (17) and (19).

Water Content Profiles:

We are primarily interested in assessing the impact of the z^2- term on the profile given by Eq. (1). The use of Eq. (1) means that at the difference of our results for I or $q,$ we do not attempt to obtain $\theta(z)$ in terms of a few simple physical parameters. Instead, we require to integrate the LHS of Eq. (1) for each value of $q,$ i.e., time. Our estimates of I and q were based on Eq. (1); hence it is important to check the accuracy of Eq. (1) in predicting $\theta(z,t)$. In this paper, we carried out the calculation of the I and q estimates first, since applying Eq. (1) requires knowing $q(t)$. This section is more of theoretical interest like Eq. (1), whereas I and q as given by Eqs. (17) and (19), using Eqs. (16) and (20) for γ_0 and γ, are simple and of greater practical interest.

For the illustration, we consider a flux q =50 cm/hr with either Eqs. (12) or (19) giving t =51.1 sec. Note that our illustration is for a short time, i.e., a large q. As shown by Eq. (2), this enhances the $M-$value and hence the impact of the z^2 term on the profile, which we try to assess. This means that without the z^2-term, we can also compare with the profile obtained at ponding with a constant flux of q =50 cm/hr, since the chosen flux is larger than k_{sat}.

Using Eq. (3) with $\theta_s=\theta_{sat}$, gives the time at ponding, $t_p=97.56$ sec., i.e., about twice the time, 51.1 sec., when q =50 cm/hr for $\theta_s=\theta_{sat}$ for all times. This, of course, is because when $\theta_s=\theta_{sat}$, q is larger than q =50 cm/hr for t <51.1 sec. and for infiltration with q =50 cm/hr, a longer time is required to accumulate a similar amount of water. At 97.6 sec., this amount of water is $I=q\ tp=1.355cm,$ whereas Eq. (4), for $\theta_s=\theta_{sat}$, gives $I=1.297cm,$ which is 4.5% less than 1.355cm due to the last small term in Eq. (4). The results are shown in Fig. 5a and with more details near the wetting front in Fig. 5b. On Fig. 5b, the slight differences between the analytical results and the numerics are visible (they are not on Fig. 5a).

If we now look at the profile, with the z^2-term, but for $I=1.355cm,$ then the time is obviously longer, 55.3 sec., and the flux smaller, 48.52 cm/hr. The two profiles for $I=1.355cm$, one with z^2 for $\theta_s=\theta_{sat}$, and one without z^2 for constant flux, q =50 cm/hr, are very close in shape. Hence, the presence of the z^2-term affects the position of the profiles significantly, by 4.5%, but not their shape. We note that the z^2-term reduces the estimate of $z,$ and the more so as z is larger making the profile more "square" as shown in the figures.

As also shown in Fig. 5a and Fig 5b, there is an excellent agreement between analytical and numerical results. The analytical results are somewhat complex and to get some physical insight in the infiltration process, we are going to use some simplifications which make the results more transparent and are still quantitatively appropriate. The constant flux profile is given subscript 1, the profiles for $\theta_s=\theta_{sat}$ are assigned 2 and * for q =50 cm/hr and for $I=1.355cm,$ respectively. To be specific, we consider the front positions, denoted with subscript f, and we see on the figure that z_{1f}, z_{2f}, and z_{*f} are close and $\left(z_{1f}-z_{2f}\right)$ is an order of magnitude smaller and $\left(z_{1f}-z_{*f}\right)$ is another order of magnitude smaller.

To the lowest order, as long as $q\theta/\theta_s$ is not too close to k, Eq. (1) shows that the fronts locations are in the vicinity of

$$z_f \simeq \int_0^{\theta_{sat}} D d\theta / \left(q-k_s\right), \qquad (21)$$

which, for the present example, equals 6.2 cm, which is roughly correct. Then,

$$z_{1f} - z_{2f} \simeq M z_f^{\,2} \tag{22}$$

or, from Eqs. (2) and (21),

$$z_{1f} - z_{2f} \simeq \frac{q/2}{\left(q-k_s\right)^2}\int_0^{\theta_{sat}}\left(1-\theta/\theta_{sat}\right)D\,d\theta \tag{23}$$

which is basically smaller than z_f by an order of $\gamma_0 q/\left(q-k_s\right) \simeq .073$ so that $z_{1f} - z_{2f} \simeq 0.45cm$, which is roughly correct (slightly too large).

The value of $\left(z_{1f} - z_{*f}\right)$, as shown in Fig. 5b, is very small. Using order of magnitude estimates (calculations available upon request) we obtain

$$\left(z_{1f} - z_{*f}\right) \simeq \left(z_{1f} - z_{2f}\right) 2\gamma. \tag{24}$$

This shows that $\left(z_{1f} - z_{*f}\right)$ is an order of magnitude less than $\left(z_{1f} - z_{2f}\right)$ as obtained numerically. For the case of Fig. 5b, Eq. (24) yields $\left(z_{1f} - z_{*f}\right) \simeq .045cm$ which is basically correct, only very slightly too small.

Conclusion:

In practice, i.e., in the field, one is primarily interested in knowing I and q as a function of time, which is why this paper is primarily devoted to finding an appropriate γ to be used in Eqs. (17) and (19). Originally (Barry et al., 1995), this third parameter was obtained by curve fitting to infiltration data. Here, we derived instead a theoretical relation in Eq. (20) giving γ in terms of soil properties so that no empirical curve fitting is necessary. Analytical and numerical results were found to be in excellent agreement using a Grenoble sand for illustration.

The method is based on Eq. (1) giving the water content, θ, as a two-term expansion in z and z^2. For the Grenoble sand illustration, we checked that the profiles, numerical and analytical, are in excellent agreement using $q(t)$ as determined in Eq. (19). We found that the z^2 – term affects primarily the position of the profile rather than its shape. Finally, we derived some very simple expressions showing the relative positions of the wetting fronts, which provide a good physical insight in the infiltration process, either under constant flux or constant water content at the surface. An interesting result is that the shapes remain very similar for both cases but positions have to be assessed carefully.

REFERENCES

1. Barry, D.A., Parlange, J.-Y., Liu, M.-C., Sander, G.C., Parlange, M.B., Lockington, D.A., Stagnitti, F., Assouline, S., Selker, J., Jeng, D.-S, Steenhuis, T.S., Li, L., Haverkamp, R., and Hogarth, W.L. (2007). Infiltration and Ponding, in *Encyclopedia of Life Support Systems*, J.A. Filar, Editor. Eolss Publishers Co., Ltd.: Oxford. p. 322-346.

2. Barry, D.A., Parlange, J.-Y., Haverkamp, R., and Ross, P.J. (1995). Infiltration under ponded conditions: 4. An explicit predictive infiltration formula. *Soil Science* 160:8-17.

3. Basha, H.A. (2011). Infiltration models for semi-infinite soil profiles. *Water Resources Research*, 47:W08516.

4. Boulier, J. F., Touma, J., and Vauclin, M. (1984). Flux-Concentration Relation-Based Solution of Constant-Flux Infiltration Equation .1. Infiltration into Nonuniform Initial Moisture Profiles. *Soil Science Society of America Journal*, *48*(2):245-251.

5. COMSOL Multiphysics, Version 3.5, COMSOL. Inc. http://www.comsol.com/.

6. Evanselides, C., Tzimopoulos, C., and Arampatzi, G. (2005). Flux-saturation relationship for unsaturated horizontal flow. *Soil Science, 170*(9):671-679.

7. Fleming, J.F., Parlange J.-Y., and Hogarth, W.L. (1984). Scaling of flux and water content relations: Comparison of optimal and exact results. *Soil Science*, 137(6):464-468.

8. Green, W.H. and Ampt, G.A. (1911). Studies on soil physics Part I – The flow of air and water through soils. *Journal of Agricultural Science*, 4:1-24.

9. Haverkamp, R., Parlange, J.-Y., Starr, J.L., Schmitz, G. and Fuentes, C. (1990). Infiltration under ponded conditions: 3. A predictive equation based on physical parameters. *Soil Science*, 149:292-300.

10. Hogarth, W. L., Lockington, D. A., Barry, D. A., Parlange, M. B., Sander, G. C., Li, L., Haverkamp, R., Brutsaert, W., Parlange, J. Y. (2011). Analysis of time compression approximations. *Water Resources Research, 47*.

11. Kunze, R.J., Parlange, J.-Y., and Rose, C. (1985). A comparison of numerical and analytical techniques for describing capillary rise. *Soil Science*, 139(6):491-496.

12. Kutilek, M. (1980). Constant-Rainfall Infiltration. *Journal of Hydrology*, *45*(3-4):289-303.

13. Parlange, J.-Y. (1972). Theory of water movement in soils: 8. One-dimensional infiltration with constant flux at the surface. *Soil Science*, 114(1):1-4.

14. Parlange, J.-Y., Lisle, I.G., Braddock, R.D. and Smith, R.E. (1982). The three parameter infiltration equation. *Soil Science*, 133:337-341.

15. Parlange, J.-Y., Hogarth, W.L., Boulier, J.F., Touma, J., Haverkamp, R., and Vachaud, G. (1985). Flux and water content relation at the soil surface. *Soil Science Society of America Journal*, 49(2):285-288.

16. Parlange, J.-Y., Barry, D.A., Parlange, M.B., Hogarth, W.L., Haverkamp, R., Ross, P.J., Ling, L., and Steenhuis, T.S. (1997). New approximate analytical technique to solve Richards' equation for arbitrary surface boundary conditions. *Water Resources Research*, 33(4):903-906.

17. Richards, L.A. (1931). Capillary conduction of liquids through porous mediums. *Physics-A Journal of General and Applied Physics*, 1:318-333.

18. Si, B. C., and Kachanoski, R.G. (2000). A new solution for water storage to a fixed depth for constant flux infiltration. *Soil Science Society of America Journal*, *64*(1):24-29.

19. Sivapalan, M., and Milly, P.C.D. (1989). On the Relationship between the Time Condensation Approximation and the Flux Concentration Relation. *Journal of Hydrology*, *105*(3-4):357-367.

20. Smith, R.E. and Parlange, J.-Y. (1978). Parameter-Efficient Hydrologic Infiltration-Model. *Water Resources Research*, 14:533-538.

21. Talsma, T. and Parlange, J.-Y. (1972). One-Dimensional Vertical Infiltration. *Australian Journal of Soil Research*, 10:143-150.

22. Triadis, D. and Broadbridge, P. (2010). Analytical model of infiltration under constant-concentration boundary conditions. *Water Resources Research*, 46:W03526.

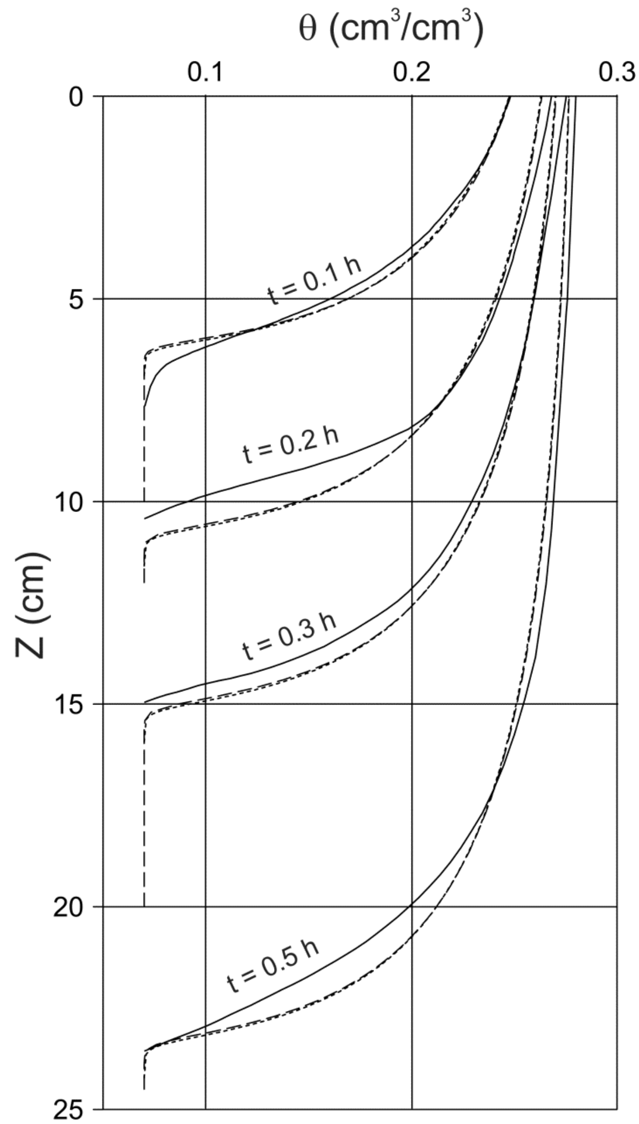

Fig. 1. Water profiles in a Grenoble sand for constant flux at the surface. The solid lines represent experimental observations (Boulier et al. 1984). The numerical predictions, dotted lines, and the analytical results from Eqs. (1) and (3) with $M = 0$, dashed lines, are essentially identical.

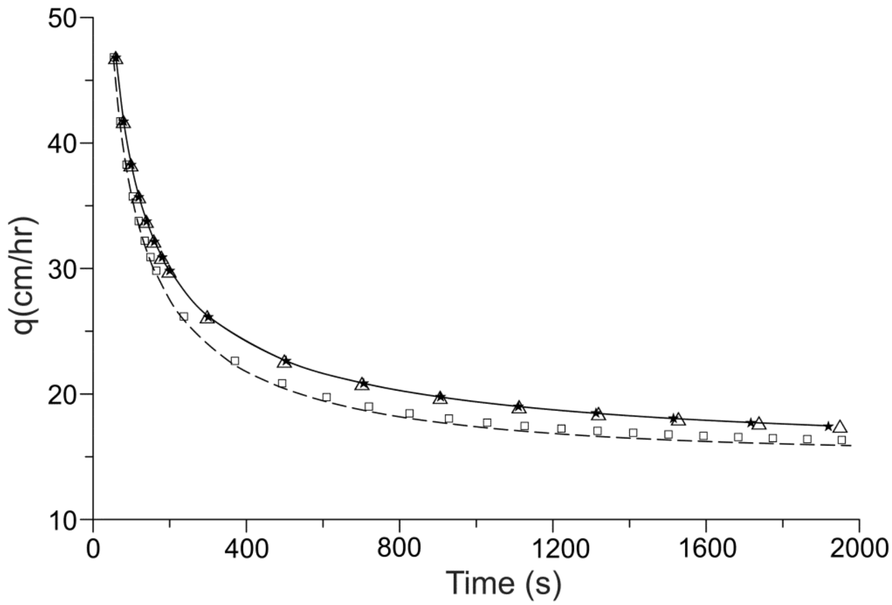

Fig. 2. Fluxes for a saturated soil surface. Numerical results (solid line) and analytical approximations: stars with Eq. (12), squares with Eq. (13), triangles with Eq. (18) and dashed line with Eq. (19). In both Eqs. (18) and (19), $\gamma = \gamma_0 = 0.05$ from Eq. (16).

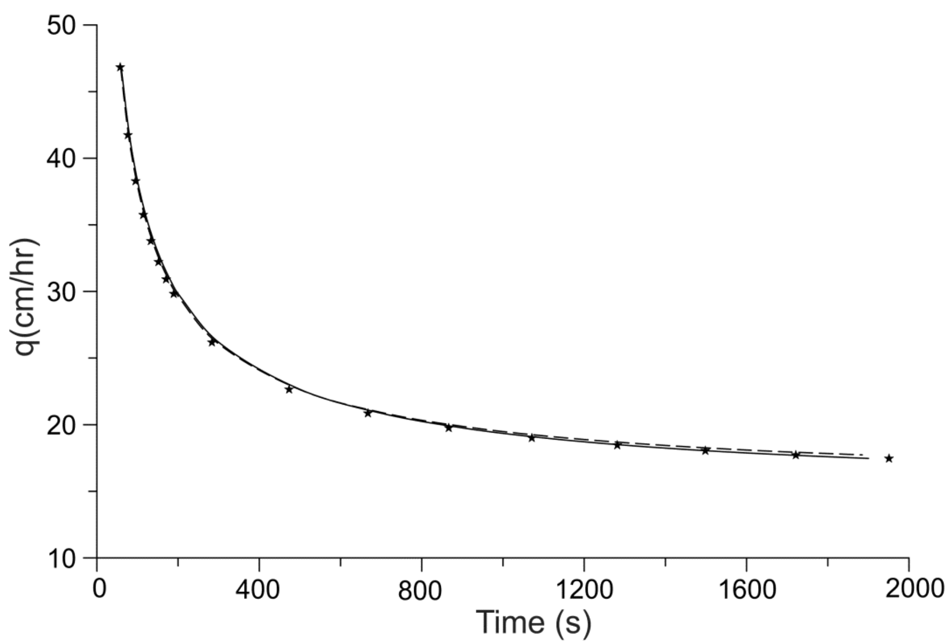

Fig. 3. Fluxes obtained numerically (solid line) and from Eq. (19): dashed line with $\gamma = 0.39$ from Eq. (20), stars with $\gamma = 0.33$ obtained by curve fitting for long times.

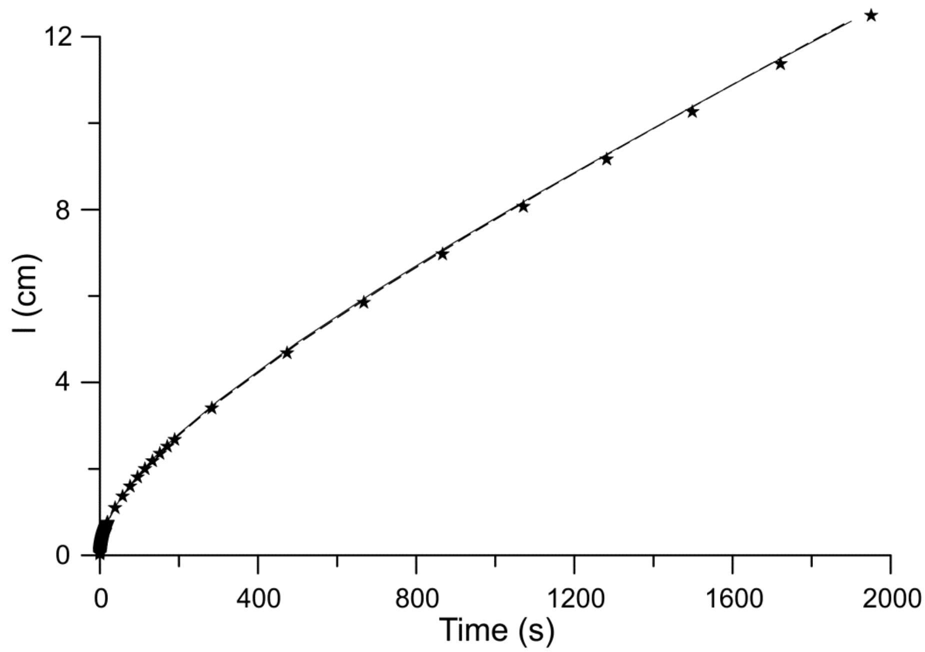

Fig. 4. Infiltration I as a function of time obtained numerically (solid line) or analytically, combining Eqs. (17) and (19) for $\gamma = 0.33$ (stars) and $\gamma = 0.39$ (dashed line).

Fig. 5. Comparison of profiles $z(\theta)$ for saturated surface and constant flux.

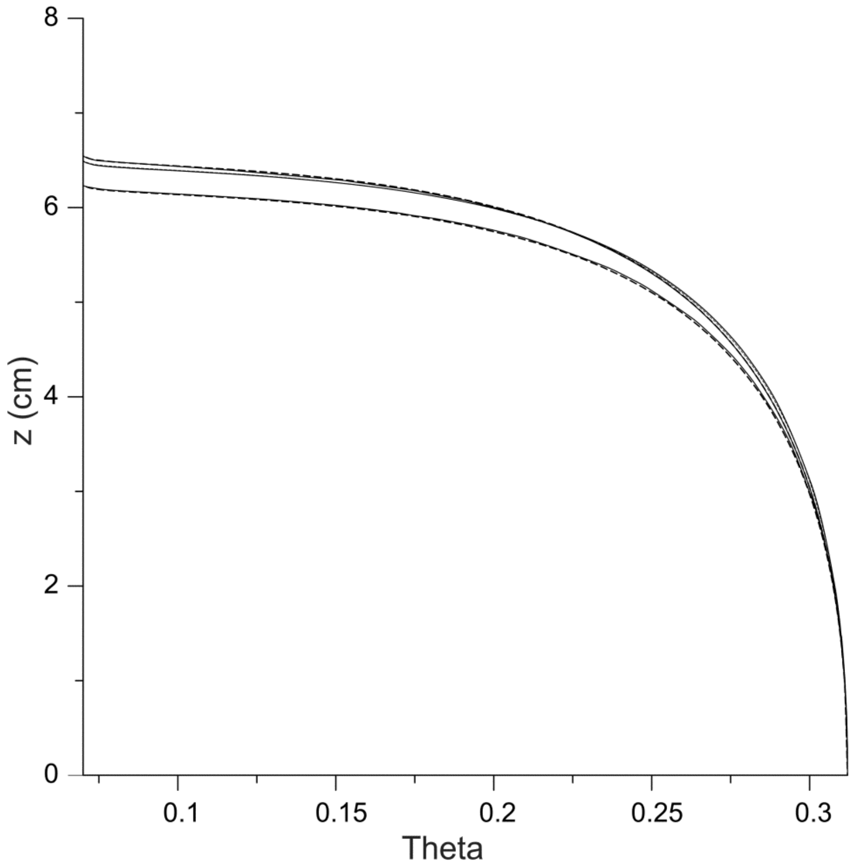

5a. Profiles over the whole range of θ, showing little difference between the numerics (solid lines) and analysis (dashed lines).

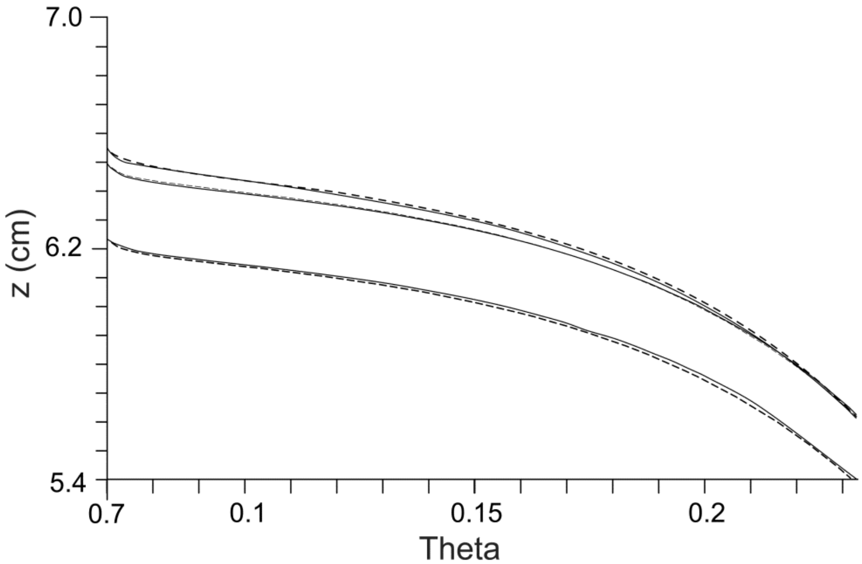

5b. Details of the profiles near the fronts. In descending order, from the top: 1. Profiles for q constant, i.e., without the $z^2 - term$, when $q = 50cm/hr$ and $I = 1.355cm$ at ponding; 2. Profiles when $\theta_s = \theta_{sat}$ at all times when $I = 1.355cm$, with the $z^2 - term$; and 3. Profiles when $\theta_s = \theta_{sat}$ at all times when $q = 50cm/hr$, with the $z^2 - term$.